Topography of ^{3}H-DHA, ^{3}H-QNB, ^{3}H-Dopamine, and ^{3}H-DAGO Binding Sites Distribution in the Central Part of the Sinoatrial Node in Rat Heart

P. V. Sutyagin, E. E. Kalinina, and A. S. Pylaev

Translated from *Byulleten' Eksperimental'noi Biologii i Meditsiny*, Vol. 140, No. 10, pp. 472-477, October, 2005
Original article submitted May 26, 2005

The topography of distribution of ^{3}H-dihydroalprenolol, ^{3}H-quinucledinyl benzilate, ^{3}H-dopamine, and ^{3}H-DAGO binding sites in the central part of the sinoatrial node in rat heart was studied by autoradiography after electrophysiological identification of the dominant pacemaker region location. Receptor asymmetry between the lateral and median regions of the central part of the sinoatrial node was shown. The dominant pacemaker region lay in the lateral area of the sinoatrial node; the number of binding sites for all four ligands was minimum in it. The number of binding sites gradually increased in the cranial and caudal directions from the dominant pacemaker region along the sinoatrial node artery (more smoothly in the caudal direction). The relative densities of bindings sites for ^{3}H-dihydroalprenolol and ^{3}H-dopamine were higher in the lateral region compared to the perinodal working myocardium, while the densities for ^{3}H-quinucledinyl benzilate and ^{3}H-DAGO were virtually the same. The distribution of binding sites along the artery in the median region of the sinoatrial node was even for ^{3}H-quinucledinyl benzilate and ^{3}H-DAGO. For ^{3}H-DAGO these parameters were close to those in the perinodal atrial myocardium, for ^{3}H-quinucledinyl benzilate somewhat lower. Curves presenting the distribution of binding site densities for ^{3}H-dihydroalprenolol and ^{3}H-dopamine in the median region of the sinoatrial node were similar, with a pronounced peak in the region contralateral to the dominant pacemaker region, and significantly higher binding parameters compared to those for the perinodal atrial myocardium. The difference consisted in higher density of ^{3}H-dopamine binding sites in the median region of the sinoatrial node in comparison with the lateral region. Binding activity was maximum in the wall of the sinoatrial node artery. The distribution of binding sites for ligands to the main autonomic nervous system neurotransmitters in the rat heart sinoatrial node is heterogeneous.

Key Words: *sinoatrial node; dominant pacemaker region; ^{3}H-dihydroalprenolol; ^{3}H-quinucledinyl benzilate; ^{3}H-dopamine; ^{3}H-DAGO*

The work of pacemaker cells (PMC), sinoatrial node (SAN), situated at the conditioned borderline of the upper (cranial) vena cava and the right auricle, ensures heart automatism in mammals. SAN in rat heart, similarly as in the majority of mammals, is situated along the artery (SAN artery) and consists of typical nodal cells forming the functional nucleus and tail of the central part and of transitional type cells forming the peripheral part [3]. The SAN region is considered to have a rich autonomic innervation [10] with a wide spectrum of neurotransmitters [8] and a high concentration of receptor structures [12]. However, treatment with basic transmitters of the autonomic nervous system (acetylcholine, catecholamines) can lead to the effect of the so-called dominant pacemaker region (PMR) migration (replacement of the leading PMC

Department of Morphology, Russian State Medical University, Moscow

0007-4888/05/1404-0468 © 2005 Springer Science+Business Media, Inc.

group by another group with a higher frequency of its own rhythm during this treatment) [1,2,12]. Moreover, sympathetic varicosities and terminals contain high levels of dopamine (catecholamine synthesis precursor), which modifies the target cells through specific dopamine receptors and through cross binding with β- and α-adrenoreceptors [7]. Enkephalins inhibiting acetylcholine and catecholamine release from the terminals [11,14] play an important role in the regulation of cardiac chronotropy.

We studied the topography and densities of binding sites for ligands to β-adrenergic receptors (^{3}H-dihydroalprenolol; ^{3}H-DHA), muscarinic cholinergic receptors (^{3}H-quinucledinyl benzilate; ^{3}H-QNB); dopamine (^{3}H-dopamine) and opiate (^{3}H-DAGO) receptors in the central part of the rat heart SAN.

MATERIALS AND METHODS

Experiments were carried out on male Wistar rats (60-90 g). The hearts were removed under Nembutal narcosis (40 mg/kg) and placed into cuvettes with Hanks medium (pH 7.35, 15-20°C), after which the right atrial region containing the anterior wall, right cranial and caudal venae cavae, and the auricle was isolated. SAN was situated at the interface between the right cranial vena cava and auricle along the SAN artery [3]. The preparation was then fixed in a frame and put into a flow termostated (38°C) cuvette with modified Krebs—Ringer solution equilibrated with 5% carbogen to pH 7.4. The rate of medium replacement in the cuvette was 1.7 ml/min. PMR was detected using glass microelectrodes. The shape of PMC action potential (slow diastolic depolarization phase, smooth transfer from slow diastolic depolarization phase into the phase of initial rapid elevation of potential, and low velocity of initial rapid elevation of potential) was the criterion of true PMC [3]. After detection of PMR the glass microelectrode was left in the tissue and culture medium in the cuvette was replaced (for 15 min) with washing medium. The media used for each ligand were described previously [4,5]. Ligand binding was carried out by replacing the washing medium by medium with ^{3}H-DHA (Amersham, 38 Ci/mmol), ^{3}H-QNB (Amersham, 30 Ci/mmol), ^{3}H-dopamine (Amersham, 49.7 Ci/mmol), and ^{3}H-DAGO (Amersham, 48 Ci/mmol) to a final concentration of the labeled ligand 1 nM for ^{3}H-QNB and 2 nM for others [6]. Binding reaction was carried out at 20-25°C for 1 h for ^{3}H-DHA, ^{3}H-dopamine, and ^{3}H-DAGO and for 2 h for ^{3}H-QNB in darkness [4,5]. Three experimental animals were used per experiment.

After the end of binding the medium in the cuvette was twice (3 min each time) replaced with washing medium and then 4% glutaraldehyde in Millonig buffer was added and the preparation was fixed for 2 h. Sketches of the SAN artery and position of the glass microelectrode were made at the end of fixation for subsequent topographic orientation of the preparation. The microelectrode was then removed from tissue, the preparation was removed from the frame, and the anterior wall of the right atrium containing the SAN region was resected under a stereomicroscope. The resected region was washed in buffer, postfixed in 1% OsO_4 in Millonig buffer, dehydrated, and embedded in Epon-812. Radioautographic study of the density of tritium label distribution was carried out on successive semithin (3 μ) sections. Blocks containing the total preparation of right atrial anterior wall were oriented so that the preparation plane maximally coincided with the plane of the resultant semithin sections, which were then mounted on slides, stained with 1% methylene blue, covered with Amersham LM-1 photographic emulsion (in darkness), dried, and exposed at 4°C. After 1 year the preparations were developed by the standard method in D-19 developer (Kodak). The images were analyzed under a Lumam-I-3 measuring microscope (objective 40). An image was projected from the microscope objective to the videocam (visual field size 26.5×32.5 μ^2). Densitometry was carried out in the immediate vicinity of the SAN arterial wall, for ^{3}H-dopamine in vascular wall. The position of microelectrode tip (PMR) served as the zero point. Then using the ocular micrometer, the preparation was shifted (with a 0.05 mm step) down the artery (along the bloodflow — positive measuring) and up the SAN artery by the same step (against the bloodflow — negative measuring). The measurements were carried out if the SAN artery wall was in the visual field. Maximum densitometry area was 0.5 mm down the SAN artery and 0.25 mm up the artery. For comparison the density of autoradiographic label in the tissue of adjacent perinodal atrial working myocardium was evaluated. The videocam images were computer-processed [4] and expressed as the percentage of visual field occupied by autoradiographic label grains. Relative density of autoradiographic label was estimated as the ratio of percentage of area occupied by the label in the examined visual field to the maximum area occupied by the label in the examined section. Curves of autoradiographic label distribution along the SAN artery were plotted for each section (Figs. 1, 2). The results were processed using Student's *t* test.

RESULTS

Comprehensive studies of the central part of the rat heart SAN showed similar distribution of binding sites for all four ligands in the lateral region occupied by a group of typical nodal cells forming PMR [4,5]. The

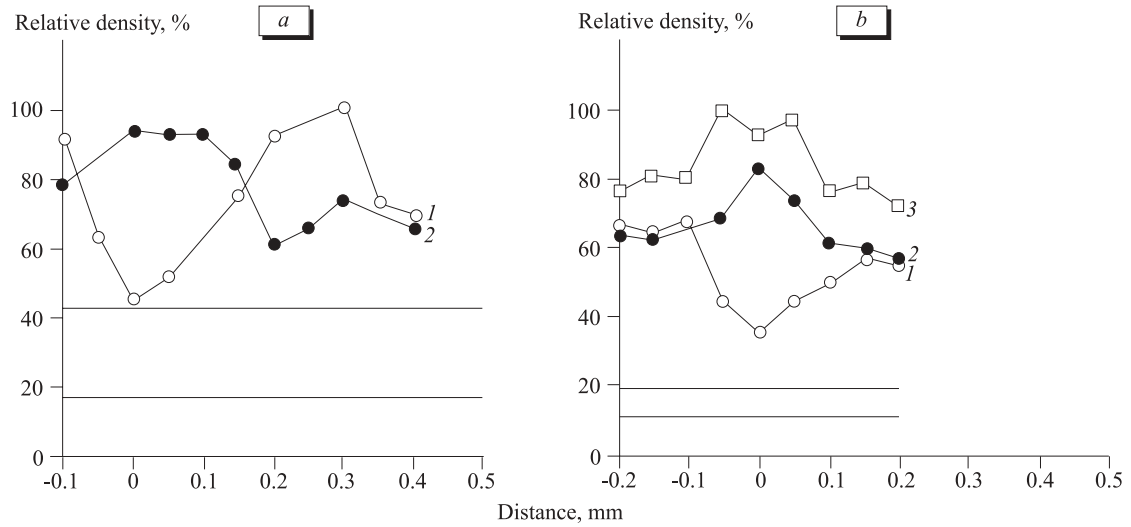

Fig. 1. Relative optical density distribution for ^{3}H-DHA (*a*) and ^{3}H-dopamine (*b*) binding sites in structures of the sinoatrial node (SAN) central part along the SAN artery in a semithin section. Here and in Fig. 2: *1*) lateral area of SAN central part; *2*) median area of SAN central part; *3*) SAN artery wall.

PMR area contains the minimum number of binding sites for the studied ligands (Figs. 1, 2, 3). The number of receptors sharply increases to the maximum values in the cranial direction and smoothly increases in the caudal direction. In some cases, when the SAN artery area in the studied section was large, the density of silver grains gradually approached the values characteristic of the perinodal atrial myocardium. The described distribution of the receptor structures in the lateral region of SAN central part is in line with the hypothesis about the receptor mechanism of the PMR migration effect in response to norepinephrine [1] and acetylcholine [2] *in vitro*. The PMR region linearly migrated in the caudal direction within the central part of SAN in response to increasing concentrations of norepinephrine in the cuvette. This migration seemed to be largely determined by positive gradient of β-adrenoreceptor density (Fig. 1, *a*) [1]. Addition of acetylcholine into cuvette did not induce PMR migration, because this region is the least sensitive to acetylcholine and hence, possesses the highest intrinsic rhythm. Migration of PMR in the cranial direction just confirms the known assumption, as PMR in these preparations is located (by physiological reasons) in the functional tail and during exposure to acetylcholine immediately returns into the functional nucleus against muscarinic cholinergic receptor gradient (Fig. 2, *a*). No relationship between the distance of PMR

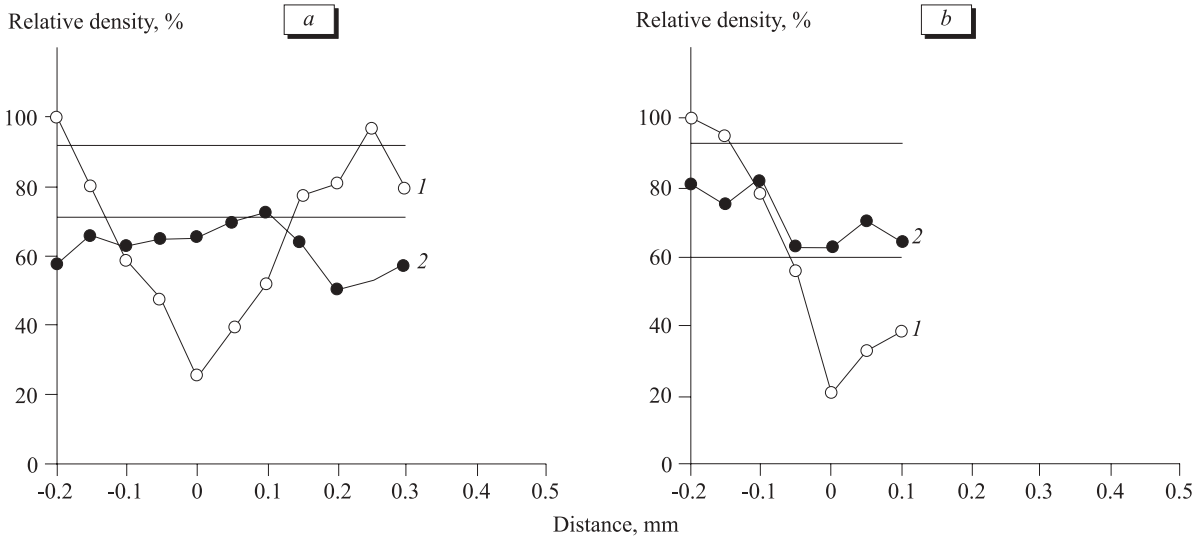

Fig. 2. Relative optical density distribution for ^{3}H-QNB (*a*) and ^{3}H-DAGO (*b*) binding sites in structures of the SAN central part along the SAN artery in a semithin section.

migration and acetylcholine concentration in the cuvette was detected [2]. The mechanism of PMR migration in canine SAN remains unclear; the PMR in dogs is characterized by maximum density of cholin- and adrenergic innervation and of the corresponding receptor structures [12].

The curve of ^{3}H-dopamine binding site density distribution in the SAN lateral region (Fig. 1, *b*) also shows the minimum values in the PMR region. The density increases in the caudal and cranial directions. However, the number of ^{3}H-dopamine binding sites in the SAN central region in comparison with the perinodal working myocardium is higher in comparison with perinodal working myocardium (15±4%, $p<0.05$) than for ^{3}H-DHA (30±13%, $p<0.05$). These facts attest to similarity between adrenoreceptor and dopamine receptor distribution in the SAN lateral region and point to additive cross-binding of ^{3}H-dopamine (dopamine receptors+β-adrecoreceptors+α-adrenoreceptors) [7].

Opioid receptors (κ and γ) detected on membranes of cholin- and adrenergic varicoses and terminals suppress acetylcholine and catecholamine release from them [11,14]. The density distribution of ^{3}H-DAGO (synthetic enkephalin analog) binding sites (Fig. 2, *b*) indirectly indicates the presumably decreased density of cholin- and adrenergic innervation of the functional nucleus. The same is confirmed by a lower number of ^{3}H-dopamine binding sites in this region, which contradicts the data of other authors [10]. However, this disagreement can presumably be explained by species characteristics of the structure of the SAN central part. These peculiarities are confirmed by facts indicating that dogs have the maximum concentration of cholin- and adrenergic structures in the central part of SAN [12], while in rats adrenoreceptor structures in SAN predominate; the presentation of cholinoreceptors was virtually the same in SAN and adjacent atrial myocardium [4].

The median region of the SAN central part seems to be a uniform formation for ^{3}H-QNB and ^{3}H-DAGO binding, quantitatively little differing from the perinodal atrial myocardium (Fig. 1, *b*; 2, *b*). The level of ^{3}H-QNB binding in the median region is low in comparison with the lateral region and adjacent atrial myocardium.

The data on the distribution of binding sites for ^{3}H-DHA (β-adrenoreceptors) and ^{3}H-dopamine along the SAN artery seem to be the most important. The density distribution curves for the lateral and median regions of the SAN central part were similar (Fig. 1, *a*, *b*). However, in a region contralateral to the PMR (Fig. 3, *b*) we observed a peak of binding of these

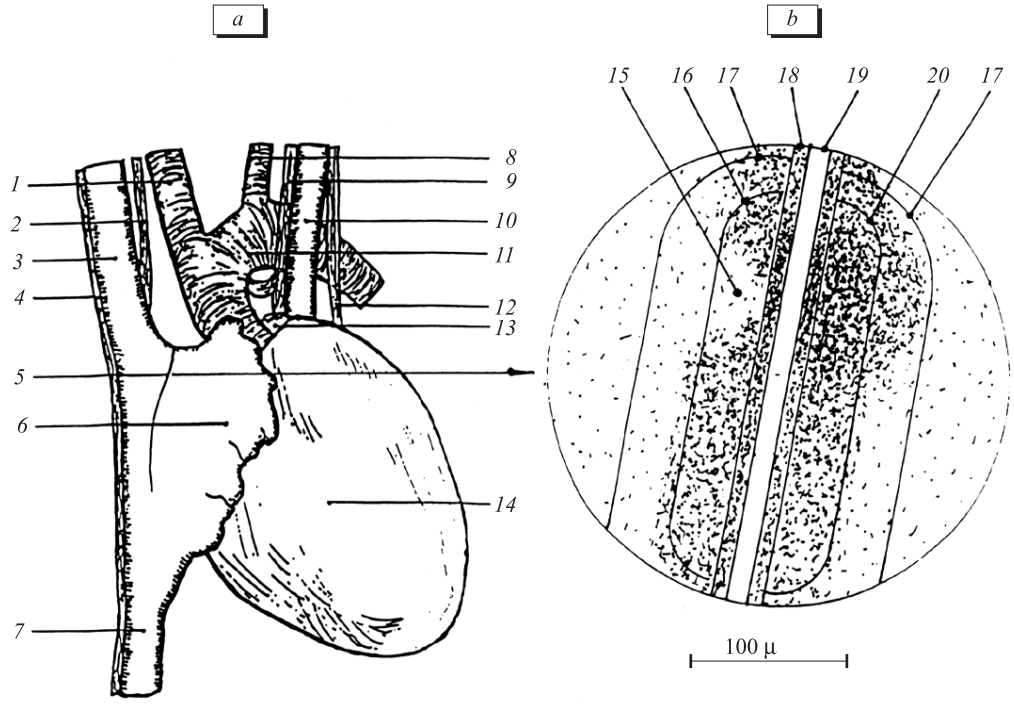

Fig. 3. Scheme of topographic location of SAN structures in rat heart. *a*) frontal aspect; *b*) fragments of SAN central part artery. Dots show distribution of autoradiographic label of ^{3}H-dopamine binding sites. *1*) *truncus brachiocephalicus*; *2*) *n. vagus dexter*; *3*) *v. cava cranialis dextra*; *4*) *n. phrenicus dexter*; *5*) SAN artery; *6*) *auricula dextra*; *7*) *v. cava caudalis*; *8*) *a. carotis communis sinistra*; *9*) *n. vagus sinister*; *10*) *v. cava cranialis sinistra*; *11*) *arcus aortae*; *12*) *n. phrenicus sinister*; *13*) *auricula sinistra*; *14*) *ventriculus dexter*; *15*) dominant pacemaker region; *16*) arbitrary border of the SAN central part lateral region; *17*) arbitrary border of SAN peripheral part; *18*) SAN arterial wall; *19*) SAN artery lumen; *20*) arbitrary border of median region of SAN central part.

ligands with gradual decrease in the number of binding sites in the caudal and cranial directions. This peak was much more expressed (in comparison with the working atrial myocardium parameters) for ^{3}H-dopamine (Fig 1, *b*). The density distribution for dopamine and adrenergic receptors in the median region of SAN central part coincided, the higher density of the ligand binding sites being determined by cross-reaction processes. No asymmetry for α_1- [13] and β-adrenoreceptors (reference in [4]) was observed in rat SAN, though the number of these receptors in SAN was higher than in working atrial myocardium. A vast accumulation of ^{3}H-dopamine binding sites was observed in the median region opposite to the initial PMR; maximum binding of ^{3}H-dopamine was registered for the SAN arterial wall (Fig. 3, *b*). Dopamine receptors detected in coronary arterial walls and in the myocardium belong to D2-like receptors [9] (to D4 subtype [7]); they are situated on varicoses and terminals of the postganglionar fibers of the autonomic nervous system and are involved in the regulation of neurotransmitters release [7]. The bulk of D2-like receptors is linked with catecholaminergic nerve fibers [9]. Thus, a potent local accumulation of adrenergic terminals regulating cardiac chronotropy (including with participation of PMR migration) was observed in the functional nucleus, similarly as in the entire central part of SAN. Cluster of ^{3}H-dopamine binding sites in an area located opposite to the functional nucleus coincided with the place of origination of SAN arterial branch, a reliable topographic landmark for the initial PMR [3]. It seems that accumulation of autonomic conductors in the SAN median region in the ontogenesis determines the location of the initial PMR in the lateral region, inducing ramification of the SAN artery.

Migration of PMR [1,2] and results of rat SAN mapping enabled us determine the length of the SAN central part as about 0.3 mm. Analysis of the ligand binding included evaluation of the functional nucleus (initial PMR) size. The pattern of ligand binding sites distribution in the SAN lateral region (Fig. 1, 2) with pronounced minimum in the initial PMR region was observed in three, maximum four successive sections. This indicates that the thickness of the initial PMR (functional nucleus) in the endoepicardial direction is about 10 μ. The minimum levels of binding were observed on a section containing the trace of the microelectrode tip; the curve pattern for the next and following sections gradually leveled until complete disappearance of the minimum. This organization of the functional nucleus rules out the possibility of direct statistical analysis, thus necessitating the study of the ligand binding sites distribution in each section. We used sections with clearly seen trace of the glass microelectrode tip (the very center of the functional nucleus; Figs. 1, 2 in [4,5]) for demonstration of the results.

Hence, the rat heart SAN is a complex structure organized along the SAN artery, with a central (functional nucleus and tail) and peripheral parts. The central part of SAN is divided by the artery into median and lateral regions, each with a specific clear-cut profile of reception. The SAN functional nucleus is situated in the lateral region and is largely devoid of receptors to the main neurotransmitters of the autonomic nervous system.

REFERENCES

1. E. E. Kalinina, P. V. Sutyagin, and A. S. Pylaev, *Byull. Eksp. Biol. Med.*, **125**, No. 3, 337-339 (1998).
2. P. V. Sutyagin, E. E. Kalinina, and A. S. Pylaev, *Ibid.*, **138**, No. 8, 218-220 (2004).
3. P. V. Sutyagin, E. E. Kalinina, and A. S. Pylaev, *Ibid.*, **139**, No. 2, 227-230 (2005).
4. P. V. Sutyagin, E. E. Kalinina, and A. S. Pylaev, *Ibid.*, **140**, No. 7, 104-108.
5. P. V. Sutyagin, E. E. Kalinina, and A. S. Pylaev, *Ibid.*, No. 8, 210-214.
6. V. N. Yarygin, V. V. Glinkina, L. A. Knyazeva, *et al.*, *Ibid.*, **109**, No. 6, 597-598 (1990).
7. F. Amenta, A. Ricci, S. K. Tayebati, and D. Zaccheo, *Ital. J. Anat. Embryol.*, **107**, No. 3, 145-167 (2002).
8. P. Beaulieu and C. Lambert, *Cardiovasc. Res.*, **37**, No. 3, 578-585 (1998).
9. C. Cavalotti, F. Nuti, P. Bruzzone, *et al.*, *Clin. Exp. Pharmacol. Physiol.*, **29**, Noû. 5-6, 412-418 (2002).
10. L. T. Chow, S. S. Chow, R. H. Anderson, *et al.*, *Anat. Rec.*, **264**, No. 2, 169-182 (2001).
11. M. Farias, K. Jackson, D. Yoshishige, *et al.*, *Am. J. Physiol.*, **285**, No. 3, H1332-H1339 (2003).
12. F. Kurogouchi, T. Nakane, Y. Furukawa, *et al.*, *Clin. Exp. Pharmacol. Physiol.*, **29**, No. 8, 666-672 (1994).
13. K. Saito, T. Suetsugu, Y. Oku, *et al.*, *Br. J. Pharmacol.*, **111**, No. 2, 465-468 (1994).
14. A. Stanfill, K. Jackson, M. Farias, *et al.*, *Exp. Biol. Med.*, **228**, No. 8, 898-906 (2003).